Effective Image Retrieval by Shape Saliences

Ricardo S. Torres, Eduardo M. Picado,
Alexandre X. Falcão
Institute of Computing
University of Campinas
CEP 13084-851, Campinas, SP, Brazil
{rtorres,eduardo.picado,afalcao}@ic.unicamp.br

Luciano F. Costa
Institute of Physics
University of São Paulo
CP 369, CEP 13560, São Carlos, SP, Brazil
luciano@if.sc.usp.br

Abstract

Content-Based Image Retrieval (CBIR) systems have been developed aiming at enabling users to search and retrieve images based on their properties such as shape, color and texture. In this paper, we are concerned with shape-based image retrieval. Here, we discuss a recently proposed shape descriptor, called contour saliences, defined as the influence areas of its higher curvature points. This paper introduces a robust approach to estimate contour saliences by exploiting the relation between a contour and its skeleton, modifies the original definition to include the location and the value of saliences along the contour, and proposes a new metric to compare contour saliences. The paper also evaluates the effectiveness of the proposed descriptor with respect to Fourier Descriptors, Curvature Scale Space and Moment Invariants.

1. Introduction

Acquisition and storage technological improvements have supported the dissemination of a large number of images. This scenario demands the creation of information systems to efficiently search images through these collections. Many Content-Based Image Retrieval (CBIR) systems have been developed aiming at supporting image retrieval based on image properties [19]. Basically, these systems are composed by an image analysis phase responsible for algorithms that manipulate image content (the objects within an image and their properties such as shape, color and texture). This manipulation results in a series of descriptors, which are sets of vectors containing distinct data types to subsume image content. These descriptors can be subsequently used to index the images and to manipulate them according to content, in an image database. One problem in this context is that different images may have similar descriptors. Thus, the goal is to design algorithms which can discriminate images, using a given distance metric. Distance metrics are part of the definition of the specification of these algorithms. They will derive image descriptors that will be close to each other when images are similar, and farther apart when images are dissimilar. In this paper, we are concerned with shape-based image retrieval. In this context, we discuss a recently proposed shape descriptor, called shape saliences [4, 20].

Consider a closed contour and a pixel discretization of the Voronoi regions of its points within a narrow band around the contour. The saliences of a shape are defined as the influence areas of its higher curvature points [4]. A contour point is considered convex if its influence area is greater outside the contour than inside it, and concave otherwise. A narrow band is used to reduce as much as possible the cross-influence of opposite parts of the contour, which come close to each other. Unfortunately, the original method is very sensitive to locate high curvature points along the contour in the case of intricate and complex shapes. We present here, a robust method to circumvent the problem which exploits the relation between the contour and its internal and external skeletons [14, 21]. On the other hand, while the cross-influence of intricate contours makes it difficult to detect high curvature points, the influence areas of those points together with their location along the contour are very important for shape-based image retrieval.

Differently than showed in [21], we present in this paper more details related to the algorithm to extract contour saliences. Furthermore, we evaluate the contour saliences using measures of CBIR domain, like precision and recall to compare it with important shape descriptors: Curvature Scale Space (CSS) [1, 18], Fourier Descriptor [11, 16] and Moment Invariants [6, 12]. The CSS descriptor is a shape descriptor, adopted in MPEG-7 standard [3], which represents a multiscale organization of the curvature zero-crossing points of a planar curve. Fourier Descriptor and Moment Invariants are widely used shape descriptors for

comparison purposes [16, 18].

This article starts by presenting an overview of two Shape Saliences extraction algorithms in Section 2: one based on the concept of Exact Dilation with Label Propagation (EDLP) [4] and another based on the Image Foresting Transform (IFT) [20]. In Section 3, the IFT is used to obtain multiscale skeletons [9], which are used to determine salience points along the contour. Section 4 evaluates the proposed shape descriptor, Fourier Descriptors, Moment Invariants, and CSS descriptor, and discusses the main results of this work. We state the conclusion and discuss our current research on shape descriptors in Section 5.

2 Shape saliences

The algorithm proposed by Costa *et al.* [4] to determine shape salience is based on the concept of *Exact Dilation with Label Propagation (EDLP)*. More formally, the EDLP of a given seed set S assigns to each image pixel t a value $C(t)$ and a label $L(t)$, which is the minimum Euclidean distance from t to S (Euclidean distance transform) and the label of its closest pixel in S (discrete Voronoi regions) respectively.

Basically, the proposed method takes the contour points as seed pixels and an EDLP algorithm [4] is performed to determine the influence area (discrete Voronoi regions) of them. The influence areas of higher curvature points, namely *salience points*, are expected to be greater than the influence areas of the other points of the shape (see Figure 1). Moreover, in the case of a contour, the influence area of a convex point (point A) is greater outside the contour than inside it, and the other way around for a concave point (point B). The influence area of each salience point relates to the aperture angle θ, illustrated in figure 1, by the formula:

$$Area = \frac{\theta \times R^2}{2}, \qquad (1)$$

where R is a dilation radius. Costa *et al.* [4] proposed to estimate the salience points by thresholding the highest influence area, computed for low values of R (e.g. 10) in order to avoid cross-influence of opposite parts which come close to each other.

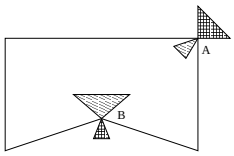

Figure 1. Internal and external influence areas of a convex (A) and a concave (B) point.

2.1 Shape saliences by image foresting transform

The shape saliences extraction algorithm, proposed in [4] can be more efficiently (in time proportional to the number of pixels) implemented by using the Image Foresting Transform (IFT) framework [10, 20]. The IFT is a recently introduced technique to the design of image processing operators based on connectivity [7–10, 15].

The *image foresting transform* (IFT) reduces image partition problems based on a given seed set to the computation of a *minimum-cost path forest* in a directed graph, whose nodes are the pixels and whose arcs are defined by an *adjacency relation* between pixels. The cost of a path in this graph is determined by a suitable *path cost function*, which usually depends on local image properties along the path — such as color, gradient, and pixel position. For suitable path-cost functions, one can choose the optimal paths so that their union is an oriented forest, spanning the whole image. The nodes of each rooted tree in the forest are by definition the influence zone of the corresponding root. The IFT assigns to each pixel three attributes: its predecessor in the optimum path, the cost of that path, and the corresponding root.

Algorithm 1 below presents the IFT procedures to compute the discrete Voronoi regions for a particular contour. Each contour pixel is considered a labeled seed. They are labeled sequentially by increasing values, starting at 1, while circumscribing the contour. This IFT generates a cost map C that outputs the squared Euclidean distance values, representing the exact dilations of the root set; a root label map L in the place of the root map which represents the influence areas of the root pixels; and the optimum-paths connecting each pixel to its corresponding root which are encoded in the predecessor map P.

Algorithm 1: Input: A contour ζ in an image I; an adjacency relation A; a labeling function λ defined on the pixel set of I which assigns subsequent integer values, starting at 1, for each contour point and 0 to the remaining pixels of I. Output: An optimum-path forest P, and the corresponding cost map C and root label map L. Auxiliary Data structures: A priority queue Q and two 2D arrays Δ_x and Δ_y that accumulate the positive increments along x and y directions.

1. For all pixels t of the image I, set $\Delta_x(t) \leftarrow +\infty$, $\Delta_y(t) \leftarrow +\infty$ and $C(t) \leftarrow +\infty$.
2. For all $t \in \zeta$, set $P(t) \leftarrow nil$, $L(t) \leftarrow \lambda(t)$, $C(t) \leftarrow 0$, $\Delta_x(t) \leftarrow 0$, and $\Delta_y(t) \leftarrow 0$ and insert t in Q.
3. While Q is not empty, do
   3.1. Remove from Q a pixel $s = (x_s, y_s)$ such that $C(s)$ is minimum.

3.2. For each pixel $t = (x_t, y_t)$ such that t is adjacent to s according to A, and $C(t) > C(s)$, do

3.2.1. Set $dx = \Delta_x(s) + |x_t - x_s|$ and $dy = \Delta_y(s) + |y_t - y_s|$.

3.2.2. Compute $C' = dx^2 + dy^2$.

3.2.3. If $C' < C(t)$, then

3.2.3.1. If $C(t) \neq +\infty$, remove t from Q. In any case, set $P(t) \leftarrow s$, $C(t) \leftarrow C'$, $L(t) \leftarrow L(s)$, $\Delta_x(t) \leftarrow dx$ and $\Delta_y(t) \leftarrow dy$. Insert t in Q.

A natural extension of this algorithm to compute contour saliences consists of obtaining a histogram of the resulting root label map for each side of the contour and restricting to a small neighborhood of the curve in order to eliminate the influence of other parts of the curve. Each bin of the histogram indicates the area of influence of the respective root inside (or outside) the contour. It is classified as *convex* when the external area is greater than the internal area, and on the other way around, it is *concave*.

Again, a point of the curve is classified as salient by thresholding its highest influence area. This approach, however, can miss important salience points in opposite parts of the shape which come close to each other. It has otherwise been particularly effective for skeletons and for simple contours, such as convex polygons, but it fails in finding the salience points of more complex and intricate contours. A robust approach to solve the problem is described next.

3 The use of skeletons for contour saliences

The proposed method for computing shape saliences uses skeleton saliences to determine contour saliences. First, a skeletonization process is performed to generate multiscale skeletons (Section 3.1); second, skeleton saliences are found (Section 3.2); and finally, the localization of contour saliences (Section 3.3) are determined. All steps are based on the IFT algorithm presented in the previous section.

3.1 Multiscale skeletonization

Given a contour with N pixels, the present method aims at assigning to each pixel inside and outside the contour the maximum length of the shortest contour segment between two roots equidistant to the pixel according to the cost map [5, 7, 9]. When a pixel has only one closest root in the contour, the assigned value is zero. This process works as follows [21].

A seed set is the labeled contour points as described in Algorithm 1 (Figure 2a). Then, Algorithm 1 is performed,

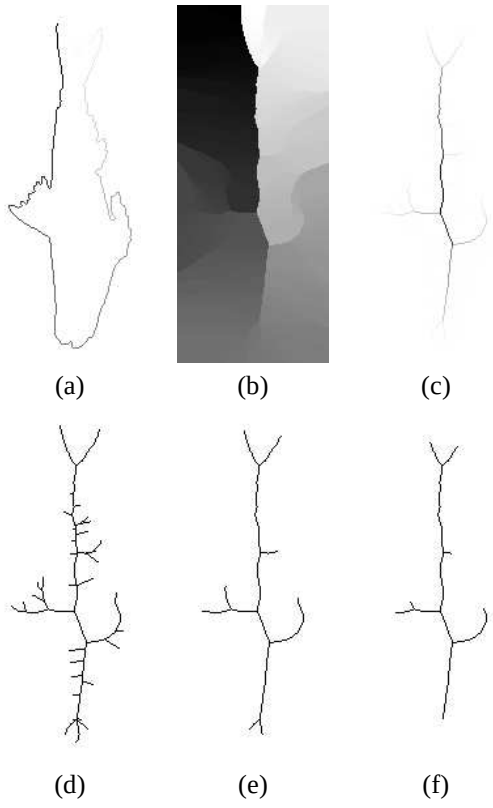

Figure 2. Multiscale skeletonization by label propagation inside a contour. (a) Labeled contour, (b) label map, (c) difference image, and (d-f) internal skeletons at three different scales.

generating a label root map L (Figure 2b). Next, a difference image D is created from L by computing the following for each pixel p inside (and outside) the contour (Figure 2c):

$$D(p) = \max_{\forall q \in N_4(p)} \{\min\{\delta(p,q), N - \delta(p,q)\}\}, \quad (2)$$

where $\delta(p,q) = L(q) - L(p)$ and $N_4(p)$ is the set of pixels q that are 4-neighbors of p. The difference image represents the multiscale internal and external skeletons by label propagation. One-pixel wide and connected skeletons can be obtained by thresholding the difference image at subsequent integer values (Figure 2d-f). The higher the threshold value, the more simplified the skeletons become, with smaller details being progressively removed as the threshold increases.

3.2 Skeleton saliences

For a given contour, multiscale skeletons are obtained as exposed in the previous section. For small scales (low

thresholds – e.g. 5% of the number of points of the contour), each salience point of the internal skeleton corresponds to one convex point of the contour and each salience point of the external skeleton corresponds to one concave point of the contour (see Figure 3). The salience points of the skeletons are determined as described in Section 2.1. Here, the skeleton points are taken as seed pixels, and the Algorithm 1 is executed for each skeleton separately, and for a small dilation radius ($R = 10$). The histogram of the root label map gives the influence areas of each skeleton point. The salience points of the skeletons are those with influence area greater than the area threshold obtained by setting $\theta = 70$ in Equation 1.

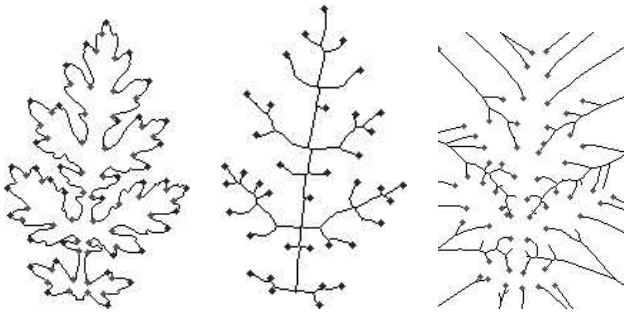

(a) (b) (c)

Figure 3. (a) Saliences of the contour of a leaf and (b-c) saliences of its internal and external skeletons.

3.3 Contour saliences via skeletons

Algorithm 1, applied to a seed set composed by the contour points, also allows a natural, simple and direct way to extract the relation between the contour and its internal and external skeletons. Equation 2 assigns to each pixel inside and outside the contour the maximum length of the shortest contour segment between two roots equidistant to the pixel according to the cost map. Figure 4a illustrates this situation for a salience point c in the skeleton, which is related to a salience point a in the contour. The difference value $D(c)$ is the length of the segment $\overline{dab}$. Suppose b is the root pixel of c in the IFT presented in Algorithm 1, the point a can be reached from the point c by skipping $\overline{dab}/2$ pixels in the anti-clockwise orientation along the contour starting from b. Similarly, the point a could be found from c through d following the clockwise orientation, when d is the root pixel of c. The method needs only to determine which is the root pixel, either b or d. If the contour pixels are labeled in clockwise orientation, the root pixel of c will be b whenever $(\delta(p,q)) > N - (\delta(p,q))$ in Equation 2 for $L(q) = L(d)$ and $L(p) = L(b)$. Otherwise, the root pixel of c will be d for $L(q) = L(b)$ and $L(p) = L(d)$. The same rule is applied for the external skeleton. Figure 4b-c illustrates the same concept applied to a real shape.

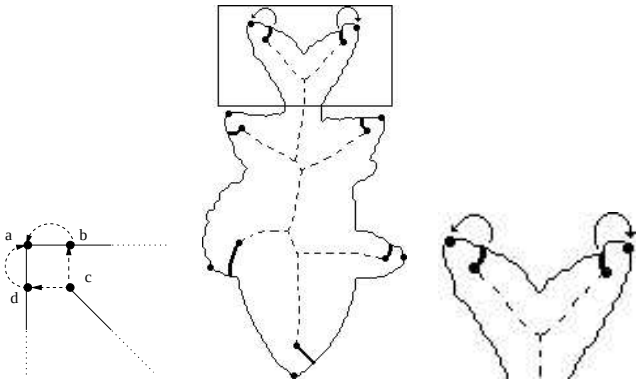

(a) (b) (c)

Figure 4. (a) Relation between skeleton and contour saliences. (b) The same concept applied to a real shape. (c) A zoomed region of Figure in (b).

The correct orientation (clockwise or anti-clockwise) is encoded in the difference image D by signaling it. To do this, Equation 2 was substituted by the following algorithm applied to all pixels p of image D:

Algorithm 2: Input: A root label map L. Output: A signed difference image D.

1. For all pixels p of image D, do
   - 1.1. Set $max \leftarrow -\infty$.
   - 1.2. For all pixels $q \in N_4(p)$, do
     - 1.2.1. Set $min \leftarrow \min\{(\delta(p,q)), N - (\delta(p,q))\}$ and $s \leftarrow 1$.
     - 1.2.2. If $min = N - (\delta(p,q))$, then
       - 1.2.2.1. Set $s \leftarrow -1$.
     - 1.2.3. If $min > max$, then
       - 1.2.3.1. Set $max \leftarrow min$ and $sign \leftarrow s$.
   - 1.3. Set $D(p) \leftarrow sign \times max$.

Although the influence areas (saliences) of the contour points do not provide a completely robust method to locate the salience points, they encode important local and global information about the contour. The saliences are also signed negative for concave points and positive for convex points. An arbitrary point of the contour is taken as reference point and the method computes the relative position

of each salience point with respect to the reference point along the contour. Finally, the proposed contour saliences descriptor consists of two vectors of the same size: one with the saliences and another with the relative position of the salience points along the contour. Note that the dimension of these vectors may be different for different contours as well as the reference points. A special algorithm has been designed for matching this descriptor between two contours taking into account these differences. This algorithm is described in Section 3.4.

Figure 5 illustrates the contour saliences descriptor for a polygon. The contour of the polygon, its reference point, the internal and external skeletons, and the respective salience points are indicated in Figure 5a. The curve shown in Figure 5b indicates the saliences by the relative position of the points along the contour.

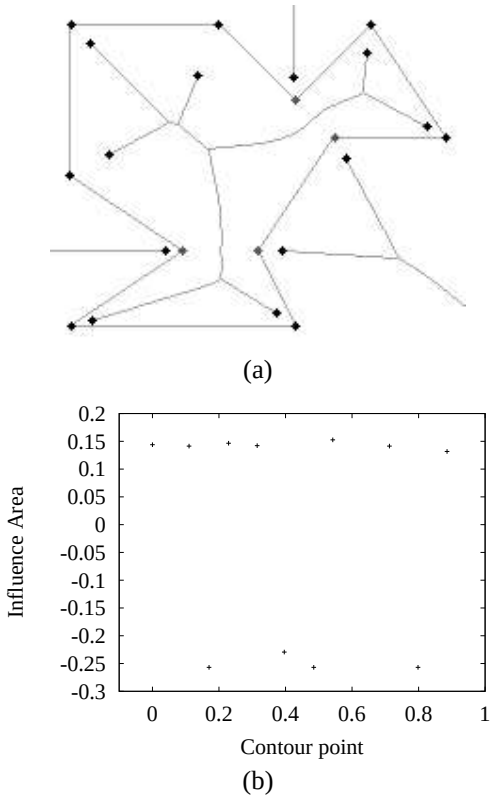

Figure 5. (a) Contour and skeletons of a polygon, where salience points are indicated by dots. (b) The salience curve of the polygon contour.

3.4 Matching algorithm for contour saliences

Whenever two contours of the same object appear in different positions and scales, they should be represented by the same salience points along the contour. Therefore the pairwise comparison between objects using contour saliences requires matching between contours.

The contour salience descriptor considered in the current work preserves the salience values of the points along the contour and their relative position regarding to a reference point. These characteristics encode a lot of information about the shape. The reference point is used only for correction of the relative positions after the matching. The matching algorithm proposed in this paper is based on the matching algorithm proposed to match Curvature Scale Space (CSS) images presented in [1, 18].

Let $S_A = \{(u_{A1}, s_{A1}), \ldots, (u_{An}, s_{An})\}$ and $S_B = \{(u_{B1}, s_{B1}), \ldots, (u_{Bm}, s_{Bm})\}$ be two salience descriptors of shapes A and B, where (u_{Ai}, s_{Ai}) stands for the i^{th} salience value s_{Ai} at the position $u_{Ai} \in [0, 1]$ along the contour of the shape A. Output: distance D.

1. Create $S'_A = \{(u'_{A1}, s'_{A1}), \ldots, (u'_{An}, s'_{An})\}$ and $S'_B = \{(u'_{B1}, s'_{B1}), \ldots, (u'_{Bm}, s'_{Bm})\}$ by sorting S_A and S_B according to the decreasing order of salience values.

2. Create a list L containing a pair of matching candidates points from S'_A and S'_B.

   A pair $((u'_{Ai}, s'_{Ai}), (u'_{Bj}, s'_{Bj}))$ belongs to the list L if $|s'_{Ai} - s'_{Bj}| \leq 0.2 s'_{A1}$. A pair $((u'_{Bj}, s'_{Bj}), (u'_{Ai}, s'_{Ai}))$ belongs to the list L if $|s'_{Bj} - s'_{Ai}| \leq 0.2 s'_{B1}$.

3. For each pair of matching candidates in the form $P_{ij} = ((u'_{Ai}, s'_{Ai}), (u'_{Bj}, s'_{Bj}))$ in L, find the shift parameter α as $\alpha = u'_{Ai} - u'_{Bj}$.

   Next, shift S_A salience points by α, yielding $S''_A = \{(u''_{A1}, s''_{A1}), (u''_{A2}, s''_{A2}), \ldots, (u''_{An}, s''_{An})\}$.

4. The distance D between S''_A and S_B is given as:

$$D = \sum_{k=1}^{\min\{n,m\}} D_k,$$

   where

$$D_k = \begin{cases} \sqrt{(u''_{Ak} - u_{Bk})^2 + (s''_{Ak} - s_{Bk})^2}, \\ \textit{if } |u''_{Ak} - u_{Bk}| \leq 0.2 \\ s''_{Ak} + s_{Bk}, \\ \textit{otherwise.} \end{cases}$$

   Finally, if $n \neq m$, it is added to D the height s of the non matched points.

5. Repeat the steps 3 and 4 by considering matching candidate pair in the form $P_{ij} = ((u'_{Bj}, s'_{Bj}), (u'_{Ai}, s'_{Ai}))$ in L.

6. Select the lowest distance D as the distance between S_A and S_B

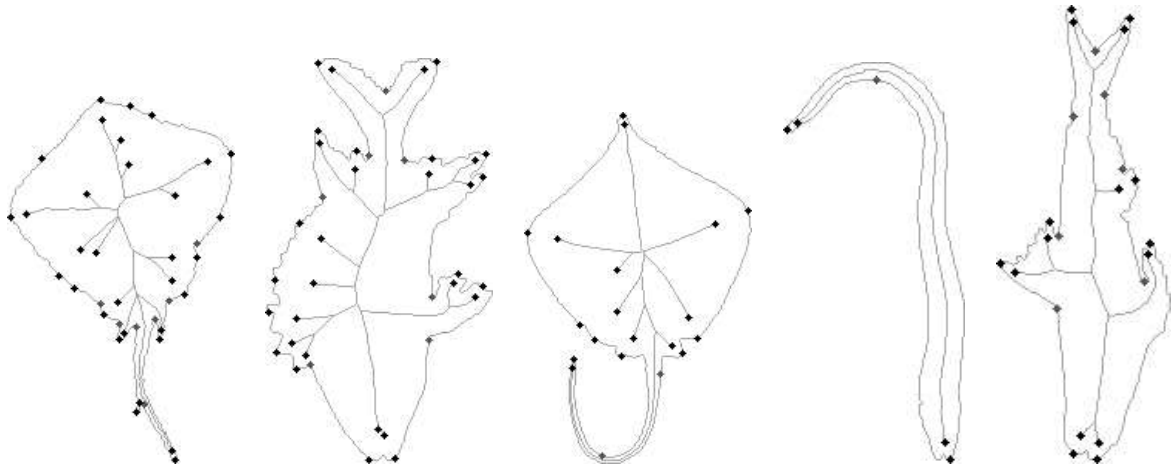

(a) (b) (c) (d) (e)

Figure 6. Fish images used for descriptor evaluation. The concave points were determined through the salience points of the external skeleton, not shown in this figure.

4 Evaluation

This section compares the proposed descriptors to commonly used shape descriptors.

4.1 Evaluated descriptors

Even though the external skeleton can be used to determine the correct location of a concave salience along a contour (see Figure 6), preliminary results showed that the contour salience presents the best behavior if we consider only the convex saliences. We have found out that the choice of the best threshold to determine the external skeleton salience is particularly sensitive with respect to the rotation and scaling transformations. In fact, different threshold values were used to estimate the concave saliences in Figure 6.

Table 1 shows the set of implemented shape descriptors. Moment Invariants, Fourier Descriptors and Curvature Scale Space have been widely used as shape descriptors [13, 18, 22]. Many versions of these methods have been proposed, but, in this work, we consider conventional implementations.

Fourier Descriptors: We have implemented the method described in [11, 16] to represent a shape with Fourier Descriptors applied to a contour. Each original object and its transformed versions have been represented by the most significant 126 components. The Euclidean distance has been used to measure the similarity between two Fourier-based representations.

Moment Invariants: For Moment Invariants, each object has been represented by a 14 dimensional feature vector, including two sets of normalized Moment Invariants [6, 12], one from object boundary and another from solid silhouette. Again, the Euclidean distance has been used to measure the similarity between different shapes represented by their Moment Invariants.

Descriptor Id	Descriptor Name
D1	Contour Saliences
D2	Fourier Descriptor
D3	Moment Invariants
D4	Curvature Scale Space

Table 1. List of evaluated descriptors.

Curvature Scale Space Descriptor: The CSS descriptor extraction algorithm is described in [1, 18]. The CSS descriptor vector represents a multiscale organization of the curvature zero-crossing points of a planar curve. In this sense, the descriptor dimension varies for different shapes, thus a special matching algorithm is necessary to compare two CSS descriptors (e.g. the algorithm presented in Section 3.4). We implemented a C version of the Matlab prototype presented in [17].

4.2 Shape database

We are using as reference a set containing one thousand and one hundred fish contours obtained from the database available at *www.ee.surrey.ac.uk/Research/VSSP/imagedb/demo.html*. Figure 6 shows some examples of fish contours and their respective skeletons.

Since there is no semantic definition of classes for the fish contours in this database, we defined a class as consisting of 10 different manifestations of each contour by rota-

tion and scaling. Then, the problem consists of 1100 classes with 10 shapes each.

4.3 Effectiveness measures

Our experiments adopted the *query-by-example (QBE)* [2] paradigm . This paradigm, in the image retrieval context, is based on providing an image as an input, extracting its visual features (e.g. contour saliences), measuring the distance between the query image and the images stored in the image database and, finally, ranking the images in increasing order of their distance of the query image (similarity).

The purpose of our experiments is to evaluate the effectiveness of the similarity-search of different descriptors in retrieving relevant images. Effectiveness evaluation is a very complex task, involving questions related to the definition of a collection of images, a set of query images, a set of relevant images for each query image, and adequate retrieval effectiveness measures. In our case, we use each original image as query image and we consider its manifestations as relevant images.

In our experiments, we use two graphical measures: Precision vs. Recall and θ vs. Recall. Precision vs. Recall ($P \times R$) curves are the commonest evaluation measure used in CBIR domain. Precision is defined as the fraction of retrieved images which is relevant to a query. In contrast, recall measures the fraction of the relevant images which has been retrieved. A recall is a non-decreasing function of rank, while precision can be regarded as a function of recall rather than rank. In general, the curve closest to the top of the chart indicates the best performance.

A $\theta \times Recall$ curve can be seen as a variation of the $P \times R$. We define θ as the average of the precision values measured whenever a relevant image is retrieved. For 100% of recall, the θ value is equivalent to the average precision. The main difference between the measures is that, unlike precision, θ value is accumulative, i.e. its computation considers not only the precision at a specific recall but also the precision at previous recall levels.

4.4 Experimental results

This section discusses our experimental results related to the effectiveness of the proposed *Contour Saliences* approach. We compare *Contour Salience Descriptor* and the CBIR approaches reviewed in Section 4.1, showing that *Contour Salience Descriptor* outperforms them. Figure 7 and Figures 7 and 8 show respectively the $P \times R$ and $\theta \times R$ curves obtained for all descriptors.

Observe that the *Contour Salience Descriptor* presents the best $P \times R$ curve (Figure 7), just having an inferior behavior for $R > 0.9$. For the $\theta \times R$ curve (Figure 8), a similar result can be verified. Again, the *Contour Salience Descriptor* outperforms the others.

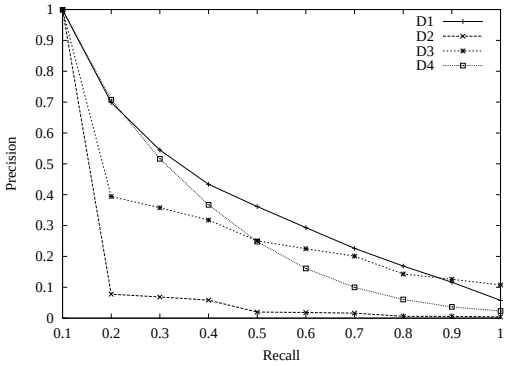

Figure 7. Precision versus Recall curve.

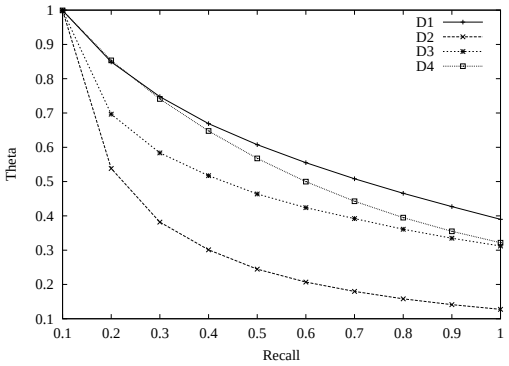

Figure 8. θ versus Recall curve.

5 Conclusion

This paper has presented an effective shape descriptor, *contour saliences*, using the framework of the IFT to encode the location and the value of saliences along the contour. The IFT provides a more efficient and more robust computation of the location of salience points as summarized in Section 3, as compared to the original algorithm published in [4]. The proposed method to locate salience points along the contour exploits the relation between contour and skeletons [14], which is naturally obtained via IFT. The contour salience descriptor, which encodes saliences and relative position of the points along the contour, and the use of a matching algorithm for it are totally new contributions.

The paper shows evaluation experiments involving the contour saliences in comparison with three broadly used descriptors, Fourier Descriptors [11, 22], Moment Invariants [6, 12] and Curvature Scale Space [1, 18]. The effec-

tiveness of the proposed descriptors is evident regarding the Precision vs. Recall and θ vs. Recall curves. The presence of manifestations, obtained by rotating and scaling operations, in the relevant sets suggests that the salience descriptor is more robust to these kind of transformations than the others. More experiments are necessary to evaluate these descriptors considering relevant sets composed by different shapes.

Ongoing developments consider the creation of shape descriptors, which combine the salience features with color- and texture-based descriptors. Moreover, we are currently considering applications in content-based image retrieval, using the proposed shape descriptors as effective indexing vectors. We also intend to incorporate concave saliences in the composition of the contour salience descriptor.

Acknowledgements

The work of R. S. Torres is supported in part by FAPESP (Proc. 01/02788-7) and the PRONEX/SAI Project (Advanced Information Systems). E. M. Picado is supported by FAPESP (Proc. 02/06907-3). A. X. Falc˜ao thanks CNPq (Proc. 302966/02-1) for financial support. The authors are grateful to Sadegh Abbasi, Farzin Mokhtarian, and Josef Kittler for the fish database.

References

[1] S. Abbasi, F. Mokhtarian, and J. Kittler. Enhancing CSS-based Rhape Retrieval for Objects with Shallow Concavities. *Image and Vision Computing*, 18:199–211, 2000.

[2] Y. A. Aslandogan and C. T. Yu. Techniques and Systems for Image and Video Retrieval. *IEEE Transactions on Knowledge and Data Engineering*, 11(1):56–63, January/February 1999.

[3] M. Bober. MPEG-7 Visual Shape Descriptors. *IEEE Transactions on Circuits and Systems for Video Technology*, 11(6):716–719, June 2001.

[4] L. da F. Costa, A. G. Campos, and E. T. M. Manoel. An integrated approach to shape analysis: Results and perspectives. In *International Conference on Quality Control by Artifi cial Vision*, pages 23–34, Le Creusot, France, May 2001.

[5] L. da F. Costa and L. F. Estrozi. Multiresolution Shape Representation without Border Shifting. *Electronic Letters*, 35(21):1829–1830, 1999.

[6] S. A. Dudani, K. J. Breeding, and R. B. McGhee. Aircraft Identifi cation by Moment Invariants. *IEEE Transactions on Computers*, c-26(1):39–45, January 1977.

[7] A. Falc˜ao and B. S. da Cunha. Multiscale shape representation by image foresting transform. In *Proceedings of SPIE on Medical Imaging*, volume 4322, pages 1091–1100, San Diego, CA, Feb 2001.

[8] A. Falc˜ao, B. S. da Cunha, and R. A. Lotufo. Design of connected operators using the image foresting transform. In *Proceedings of SPIE on Medical Imaging*, volume 4322, pages 468–479, San Diego, CA, Feb 2001.

[9] A. Falc˜ao, L. da F. Costa, and B. da Cunha. Multiscale Skeletons by Image Foresting transform and its Applications to Neuromorphometry. *Pattern Recognition*, 35(7):1571–1582, Apr 2002.

[10] A. Falc˜ao, J. Stolfi , and R. Lotufo. The Image Foresting Transform: Theory, Algorithms, and Applications. *IEEE Trans. on Pattern Analysis and Machine Intelligence*, 2003. To appear.

[11] R. C. Gonzalez and R. E. Woods. *Digital Image Processing*. Addison-Wesley, 1992.

[12] M. K. Hu. Visual Pattern Recognition by Moment Invariants. *IRE Transactions on Information Theory*, 8:179–187, 1962.

[13] A. K. Jain and A. Vailaya. Shape-based Retrieval: A Case study with trademark Image Databases. *Pattern Recognition*, 31:1369–1390, 1998.

[14] M. Leyton. Symmetry-Curvature Duality. *Computer Vision, Graphics, and Image Processing*, 38:327–341, 1987.

[15] R. Lotufo and A. Falc˜ao. The ordered queue and the optimality of the watershed approaches. In *Mathematical Morphology and its Applications to Image and Signal Processing*, volume 18, pages 341–350. Kluwer Academic, Palo Alto, USA, Jun 2000.

[16] B. M. Mehtre, M. S. Kankanhalli, and W. F. Lee. Shape Measures for Content Based Image Retrieval: A Comparison. *Information Processing and Management*, 33(3):319–337, 1997.

[17] C. Y. Ming. Shape-Based Image Retrieval in Iconic Image Databases. Master's thesis, Chinese University of Hong Kong, June 1999.

[18] F. Mokhtarian and S. Abbasi. Shape Similarity Retrieval under a Affi ne Transforms. *Pattern Recognition*, 35(31-41), 2002.

[19] A. W. M. Smeulders, M. Worring, S. Santini, A. Gupta, and R. Jain. Content-Based Image Retrieval at the End of the Years. *IEEE Transactions on Pattern Analysis and Machine Intelligence*, 22(12):1349–1380, December 2000.

[20] R. Torres, A. Falc˜ao, and L. Costa. Shape description by image foresting transform. In *14th International Conference on Digital Signal Processing*, pages 1089–1092, Santorini, Greece, Jul 2002.

[21] R. S. Torres, A. X. Falc˜ao, and L. F. Costa. A Graph-based Approach for Multiscale Shape Analysis. Technical Report IC-0303, Institute of Computing, University of Campinas, January 2003. Submitted to Pattern Recognition journal.

[22] T. P. Wallace and P. Wintz. An Effi cient Three-dimensional Aircraft Recognition Algorithm Using Normalised Fourier Descriptors. *Computer Graphics Image Processing*, 13:99–126, 1980.